HiSST: 2nd International Conference on
High-Speed Vehicle Science Technology
11–15 September 2022, Bruges, Belgium

CFD OF AXIS SYMMETRIC AFT WALL ANGLE CAVITIES IN SCRAMJETS

Naresh Relangi[1a], Antonella Ingenito[1b], Jeyakumar S[2]

Abstract

The interest in hypersonic flights lies in the possibility of reaching antipodal terrestrial distances in about a couple of hours at Mach 8. To make this technology ready, some issues still need to be addressed. At supersonic flight speeds, the air residence time is of the order of 1 millisecond: fuel and air must be mixed and burned completely in a very short time. The flow field within the combustor of the scramjet engine is very complex and poses a considerable challenge in the design and development of a supersonic combustor with optimized geometry. This combustor must promote sufficient mixing of fuel-air and flame stabilisation avoiding excessive pressure losses and consequently penalties in thrust efficiency. Therefore, the development of scramjet engines poses considerable challenges and requires multidisciplinary design, analysis, modeling, simulation and system optimization. Several studies have been carried out worldwide, and various concepts have been suggested for scramjet combustor configurations to overcome the limitations given by the short flow residence time. In this paper, performance of an innovative axisymmetric configuration has been numerically investigated by means of LES. Results show that a combustion efficiency of 80% may be attained assuming an upstream injection into the cavity.

Keywords: *Scramjet, Axisymmetric aft wall cavity, LES, Fueling technique, Vortex Shedding, Wall Pressure, Combustion Efficiency.*

Nomenclature

M – Mach number
P_o – Total Pressure (bar)
P – Static Pressure (bar)
T_o – Total Temperature (K)
T – Static Temperature (K)
YH2 – Mass fraction of Hydrogen
YO2 – Mass fraction of Water
ρ – Density (kg/m3)
u – Velocity (m/s)

1. Introduction

Mixing of air and fuel at high velocity and low residence time in scramjet engines requires the investigation of innovative injection systems or combustor geometry configurations in order to improve the flame anchoring and consequently the combustor performance [1, 2, 3].

The use of cavities for flame stabilization in a supersonic solid fuel combustor was performed primarily by Ben Yaker et al. In his work, he revealed the sustained combustion and auto-ignition of polymethylmethacrylate (PMMA) for supersonic entry conditions. Yu and Schadow experimentally demonstrated the use of cavities to excite supersonic jets. The effect of three-dimensional cavities in the supersonic flow field reveals that the width of the cavity plays an important role in increasing mixing

[1] *University of Rome "La Sapienza", 00138, Rome, Italy, relanginaresh1996@gmail.com, antonella.ingenito@uniroama1.it*
[2] *CFD center, Aeronautical Engineering, Kalasalingam Academy of Research and Education, Krishnankoil, India, sjeyakumar1974@gmail.com*

by generating turbulence. Cavities with inclined stern wall produce high strength due to the increased recompression of the cutting layers on the back wall. The effect of back pressure and cavity length-to-depth ratio (L/D) on the flow field of the scramjet combustor for non-reacting flow was computationally studied by Huang, et al. Again Kim, et al performed computational analyses of combustion improvement using cavity flame support to study the effects of stern wall angle, cavity length, depth on pressure loss, and combustion efficiency. Cavities with specific geometry can improve mixing and flame anchoring in scramjet combustors, allowing active recirculation and stable combustion within the cavity avoiding prohibitive pressure losses. The existence of recirculation area inside the cavities enhances the combustible mixture's residence time and thus cavities are preferable candidates for flame holding. The flow field inside a cavity is characterized by recirculating flow that increases the residence time of the fluid entering the cavity. Because the drag associated with flow separation is much less over a cavity than for a bluff-body, a cavity inside a combustor makes a stable flame holder with relatively little pressure drop. The velocities in these regions are equivalent to subsonic and will be helpful to draw the available fuel into them. Thus, vortex formation or creation of subsonic regions is essential in the combustor and it can be accomplished by employing various injection strategies and flame holding devices. To improve the mixing of fuel and air, various fueling techniques such as wall injectors, ramp injectors, struts, hyper mixers and cavity injection have been investigated. Higher fuel injection angles, such as cross-flow injection, allow the fuel jet to interact with the core flow, improving mixing and forming low-speed regions in the wake of the fuel jet. This strong interaction, however, will cause normal/strong oblique shocks, resulting in greater stagnation pressure losses. Lowering the fuel injection angle, on the other hand, can reduce the total pressure loss, but weakens the fuel-air interaction. As a result, there must be a trade-off between the location or angle of the fuel injector and the loss of stagnation pressure (Relangi, 2021) [4, 5, 6].

Moradi et al. [7] studied numerically the effect of cavity's shape on the fuel-air mixing in a combustor by injecting hydrogen. Following investigations on various geometrical shapes, it was discovered that the trapezoidal shape cavity produced the best results because it allows for stable and wider ignition regions. In addition, to understand an optimal location to inject fuel into a cavity combustor, the researchers conducted a series of investigations. And it is possible to feed the cavity-based combustor in two ways such as direct injection and passive injection. In case of angled injection upstream of the cavity, fuel-air mixing is more efficient as the fuel jet separates the boundary layer and allows the cavity to act as an excellent flame holder accompanied by a lower total pressure loss [8, 9]. On the contrary, injecting fuel directly into the cavity, that is, into subsonic regions, will increase the residence time of the fuel to mix well with the air and eventually produce greater combustion efficiency. Fuel injection upstream of the cavity was found to result in a greater depth of penetration into the core flow, larger recirculation regions within the cavity, and a low stagnation pressure loss profile. Since this is an extension of previous research [5, 6, 10, 11] he interest in injecting fuel into a circular combustor accompanied by assisimmetric cavities remains the same. Feeding hydrogen upstream of the cavity and through the back wall of the cavity is the main object of this research and to understand the effect on the flow field and significant performance parameters under unstable conditions, large eddy simulations at 30 km, Mach 6.8 flight conditions, were employed.

2. Simulation Setups

Fig. 1 illustrates the geometric dimensions of the combustor. The combustor has an overall length of 135 mm and is connected to an insulator 30 mm long and the same diameter as the combustor, that is, 26 mm. To minimize the effect of thermal chocking, the combustor was given a 3° divergence from 5 mm upstream of the cavity. The stern ramp of the cavity is divided into two corners of 30° and 15° to extend the mixing layer and recirculation zones. Each injector has a diameter of 1 mm and four injectors are equally spaced 90° to feed the combustor. Boundary conditions at the combustor inlet are reported in Table 1.

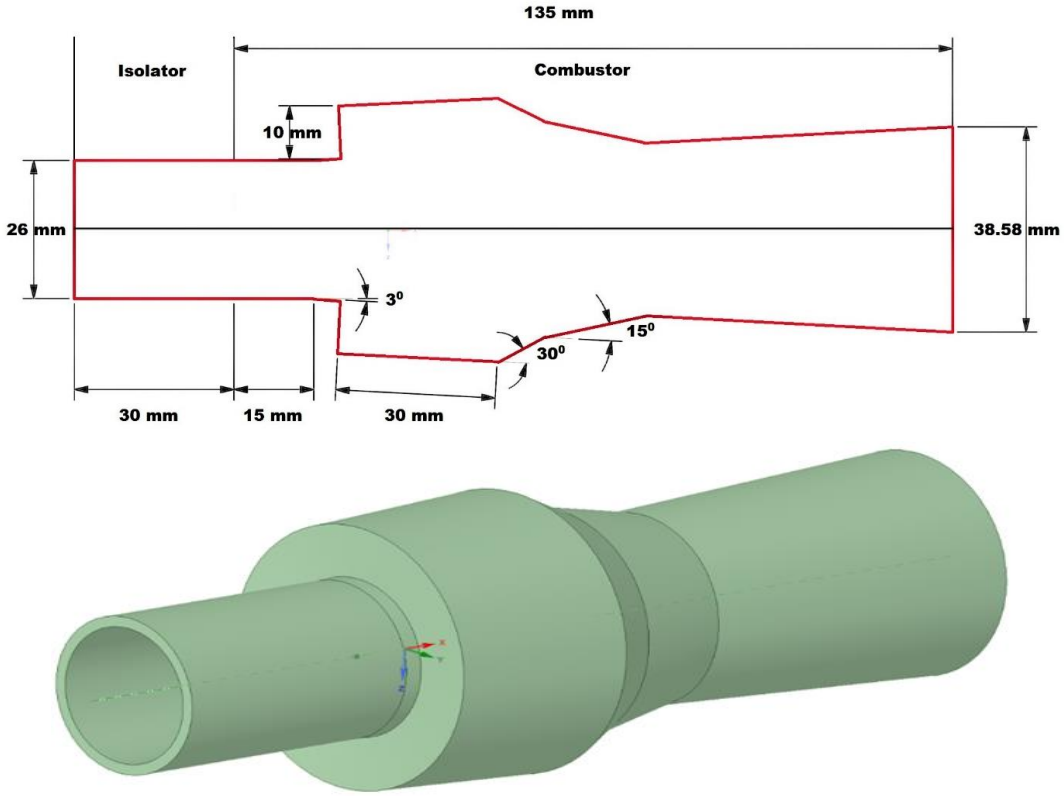

Fig 1. Schematic picture of the combustor

Table 1. Boundary Conditions

Variable	Air	H2
Po (bar)	16.56	17.5
To (K)	2254	250
M	2.8	1
YO2	0.232	0
YH2	0	1
YH2O	0.032	0

2.1. LES Transport Equations

In LES each turbulent field variable is decomposed into a resolved and a subgrid-scale part. In this work, the spatial filtering operation is implicitly defined by the local grid cell size. Variables per unit volume are treated using Reynolds decomposition, while Favre (density weighted) decomposition is used to describe quantities per mass unit. The instantaneous small-scale fluctuations are removed by the filter, but their statistical effects remain inside the unclosed terms representing the influence of the subgrid scales on the resolved ones. Gaseous combustion is governed by a set of transport equations expressing the conservation of mass, momentum and energy, and by a thermodynamic equation of state describing the gas behavior. For a mixture of Ns ideal gases in local thermodynamic equilibrium but chemical non-equilibrium, the corresponding filtered field equations (extended Navier-Stokes equations) are:

Transport equation of Mass

$$\frac{\partial \bar{\rho}}{\partial t} + \frac{\partial \hat{\rho} \tilde{u}_i}{\partial x_i} = 0 \tag{1}$$

Transport equation of Momentum

$$\frac{\partial(\bar{\rho}\tilde{u}_j)}{\partial t} + \frac{\partial(\bar{\rho}_i\tilde{u}_j + \bar{p}\delta_{ij})}{\partial x_i} = \frac{\partial\tilde{\tau}_{ij}}{\partial x_i} + \frac{\partial\tau_{ij}^{sgs}}{\partial x_i} \quad (2)$$

Transport equation of Total Energy (Internal + Mechanical)

$$\frac{\partial(\bar{\rho}\tilde{U})}{\partial t} + \frac{\partial\left(\bar{\rho}\widetilde{u_i}\tilde{U} + \bar{p}\tilde{u}_i + \bar{q}_i - \tilde{u}_j\bar{\tau}_{ij} + H_i^{sgs} - \sigma_i^{sgs}\right)}{\partial x_i} = 0 \quad (3)$$

Transport Equation for NS Species mass fractions

$$\frac{\partial(\bar{\rho}\tilde{Y}_n)}{\partial t} + \frac{\partial(\bar{\rho}\tilde{u}_j\tilde{Y}_n)}{\partial x_i} = \frac{\partial}{\partial x_i}\left[\bar{\rho}\left(D_n + D_{t,n}\right)\frac{\partial\tilde{Y}_n}{\partial x_i}\right] + \bar{\rho}\tilde{\omega}_n \quad (4)$$

Thermodynamic Equation of State

$$\bar{p} = \bar{\rho}\sum_{i=1}^{N,}\frac{\tilde{Y}_i}{W_i}\mathcal{R}_u\tilde{T} \quad (5)$$

These equations must be coupled with the constitutive equations which describe the molecular transport. In the above equations, *t* is the time variable, ρ the density, *uj the* velocities, t_{ij} the viscous stress tensor, and $\tilde{U}$ the total filtered energy per unit of mass, that is sum of the filtered internal energy, $\tilde{e}$, the resolved kinetic energy, $1/2(\widetilde{u_i u_i} - \tilde{u}_i\tilde{u}_i)$, and the subgrid one, $1/2(\widetilde{u_i u_i} - \tilde{u}_i\tilde{u}_i)$, *qi* is the heat flux, *p* the pressure, *T* the temperature. The stress tensor and the heat-flux are respectively.

$$\bar{\tau}_{ij} = 2\mu\left(\widetilde{S_{ij}} - \frac{1}{3}\widetilde{S_{kk}\delta_{ij}}\right) \quad (6)$$

$$\bar{q}_i = -k\frac{\partial(\tilde{T})}{\partial x_i} + \bar{\rho}\sum_{n=1}^{N_x}\widetilde{h_n Y_n V_{i,n}} + \sum_{n=1}^{N_x} q_{i,n}^{sgs} \quad (7)$$

Dn is the n[th]-species diffusion coefficient, *Wn* the n[th] species molecular weight, *Yn* the mass fraction, w_n is the production/destruction rate of species *n*, diffusing at velocity $V_{i,n}$ and resulting in a diffusive mass flux *Jn*. Finally, *Ru* is the universal gas constant. Summation of all species transport equations (24) yields the total mass conservation equation (21). Therefore, the *Ns* species transport equations (24) and the mass conservation equation (21) are linearly dependent and one of them is redundant. Furthermore, to be consistent with mass conservation, the diffusion fluxes ($\boldsymbol{J_n} = \rho Y_n \boldsymbol{V_n}$) and chemical source terms must satisfy.

$$\sum_{n=1}^{N_s} J_n = 0 \text{ and } \sum_{n=1}^{N,}\dot{\omega}_n = 0 \quad (8)$$

In particular, the constraint on the summation of chemical source terms derives from mass conservation for each of the*NS* chemical reactions of a chemical mechanism. The sub grid scales are modelled using Smagorinsky-Lilly model [12]. The eddy viscosity being modelled as $\nu_t = C\Delta^2\sqrt{2\bar{S}_{ij}\bar{S}_{ij}} = C\Delta^2|\bar{S}|$. Here Δ is the size of the grid and C is the constant.

The commercial code Ansys FLUENT-19.0 is used to perform the numerical analysis. The density-based solver with Implicit filter, i.e., second order implicit equation is considered to in order to eliminate excessive computational cost (sub filter scale model term). Single step reaction mechanism (fuel-air) is used and the turbulence-chemistry coupling addressed by eddy dissipation model.

$$2H_2 + O_2 \rightarrow 2H_2O \quad (9)$$

2.2. Grid Independence Study and Validation

A grid independence study was performed with three kinds of structured grids with mesh counts of M1 = 953639, M2 = 1231599, and M3 = 1458698 in order to optimize grid size. The mean static pressure along the center line of the combustor is used to check the accuracy. Seeing as there is only a 1% difference between M2 and M3 values (see fig 2). Given the economical computation cost and the good accuracy of the results, the grid M2 with 1231599 elements was preferred for the current analysis.

The numerical results have been validated with experimental data [

13], as shown in Fig. 2b. A very good agreement of the wall pressure all along the combustion chamber is shown

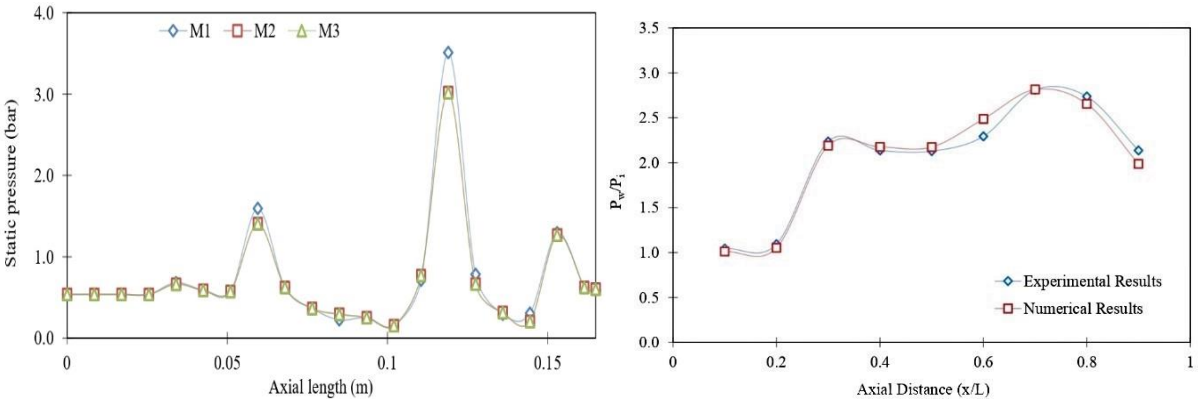

a) Normalized Pressure vs Axial Length b) Static Wall Pressure vs Axial Length

Fig 2. Static Pressure vs Axial Length

3. Results and Discussion

In this work, upstream/passive injection has been examined by means of Large Eddies Simulations in order to analyze the performance of the combustion chamber for this configuration. Fig. 5 shows the Mach number flow field. The fuel is injected with an angle of 30°, at 10 mm before the cavity. The H2 injection allows the formation of a bow shock upstream 12 mm the fuel injection. There, the Mach number decreases from 2.4 to 1.6. Oblique shocks waves reflect and interact within the core jet. Due to the increase in pressure upstream of the bow impact, the boundary layer separates, generating a turbulent region in which the flow is subsonic.

A Mach disc downstream of the cavity is shown at X = 13 mm. As the inflow enters the expansion region, the Mach number increases to 3.8 before decreasing to 1.2 after passing over the back wall of the cavity. A thermal choking is visible after the bottom wall of the cavity. Once the flow begins to move up the back wall of the cavity, it has begun to expand again. However, since there is almost no combustion in the central region, the flow remains supersonic throughout the combustor in both cases. Furthermore, gradients in the Mach number can contribute to considerable pressure drops.

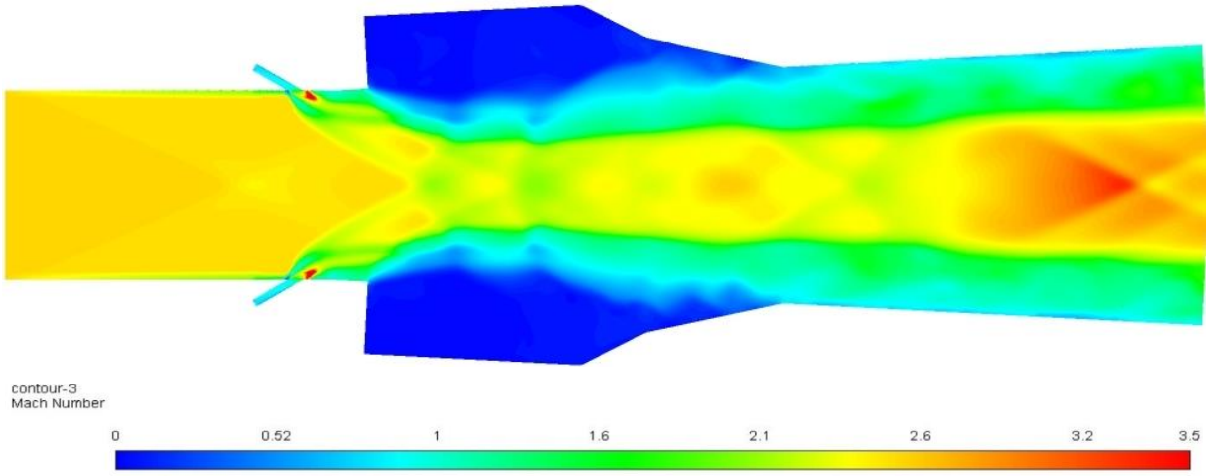

Fig 1. Mach number instantaneous contour at 50 ms

3.1 Density Contour

The density gradients are shown in Fig. 6: it shows the effect of fuel injection on a density gradient in the flow-field. A diamond structure for the oblique shock waves is visible. The shock waves are reflected from the upper and lower boundary layer and interact each other's causing the Mach disc formation. Expansion and compression waves interact within the flow field.

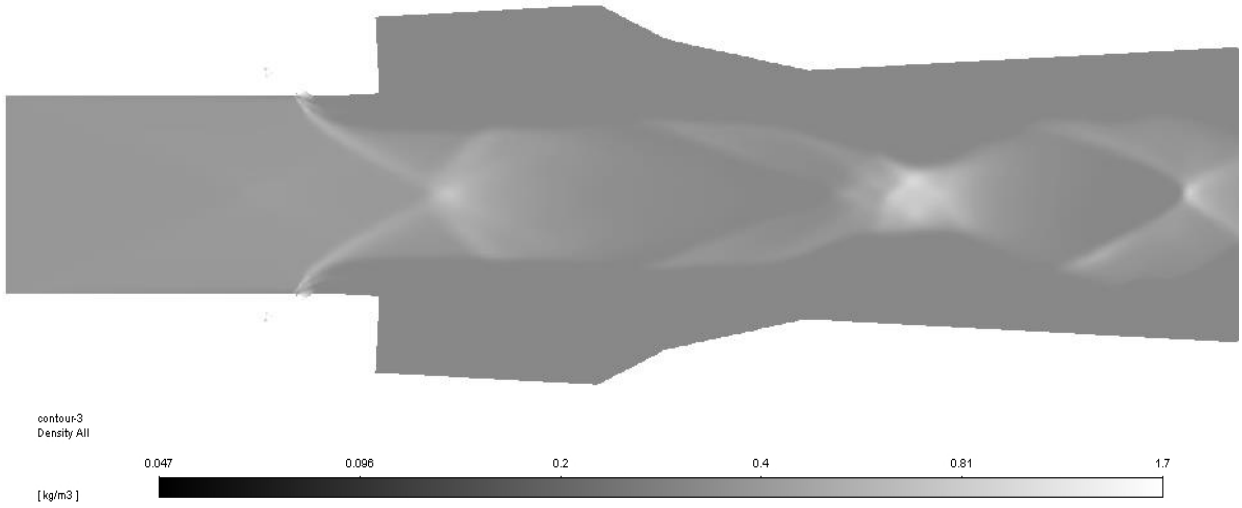

Fig 6. Density contour at 50 ms

3.2 H2 Mass Fraction

In Fig. 7, the instantaneous and averaged results of fuel distribution are shown alongside the streamlines. The fuel mass fraction is a critical parameter for understanding fuel-air mixing and combustion efficiency. Within the cavity the flow is subsonic, and spanwise vortexes generate within the cavity improving the fuel air mixing. The vortices completely occupy the entire cavity, transporting hydrogen inside the cavity. Since the presence of the cavity induces subsonic regions, it is possible to exploit these regions for mixing of fuel-air and for the flame-holding characteristics. Due to the boundary layer separation in this case, the majority of the fuel is in the mixing layer or shear layer and is being entrained into the cavity. And it will yield grater mixing efficiencies.

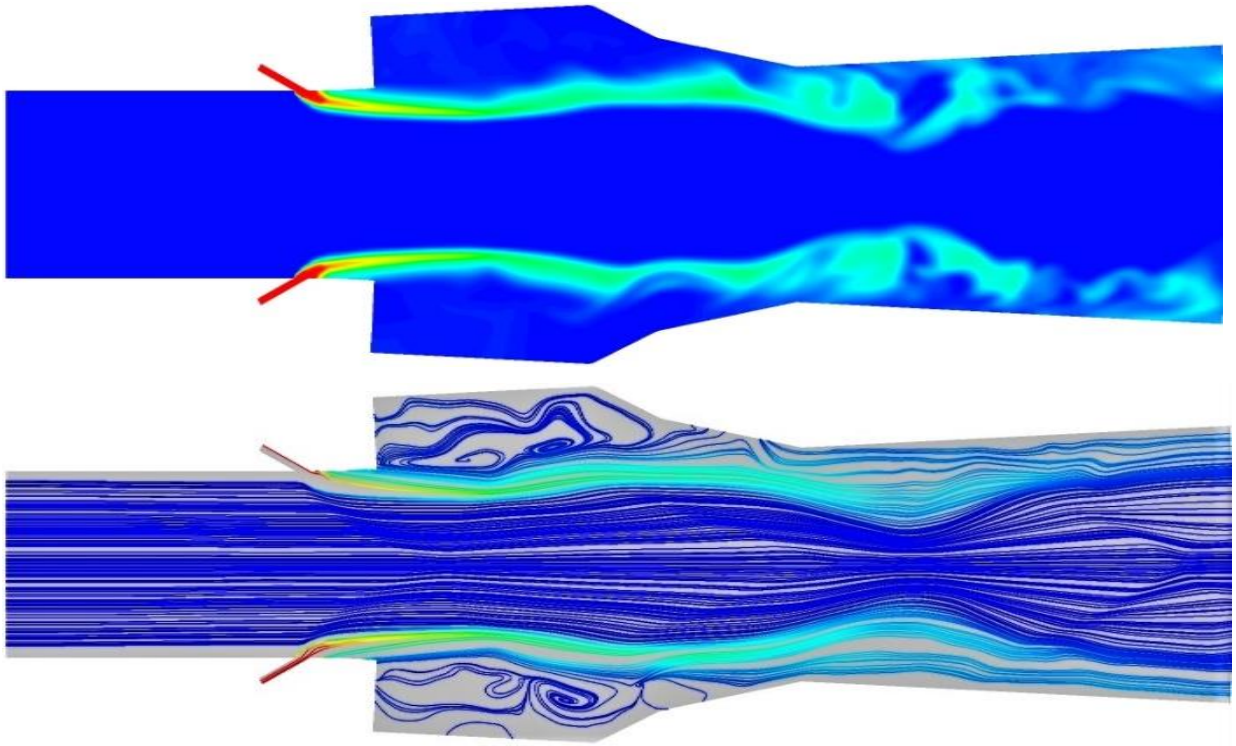

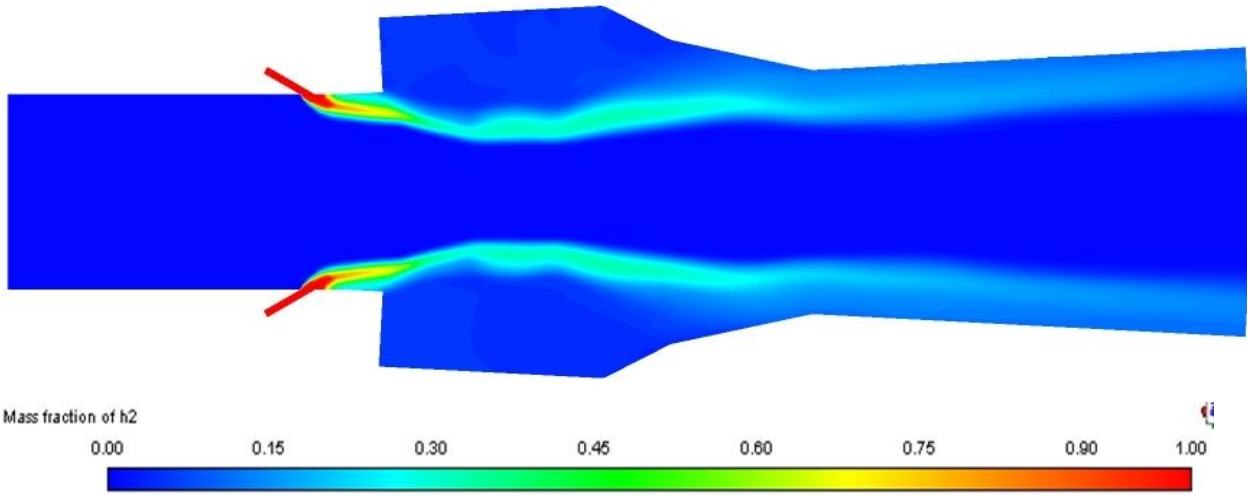

Fig 7. Instantaneous, streamlines and averaged H2mass fraction contour at 50 ms

3.3 Mean Temperature

Fig .8 shows the time-averaged static temperatures. In this case, the available fuel in the mixing layer is entrained into the cavity to react with air, resulting in intense heat release and greater combustion. The hot combustion products in the cavity zone interact with the fuel in the shear layer, anchoring the flame for the upcoming mixture. As there is good combustion within the cavity, the average temperature is around 2700 K. As the vortex (Fig. 9) moves downstream of the cavity, heat is released downstream of the cavity, specifically towards the core flow, with average temperatures around 1550 K.

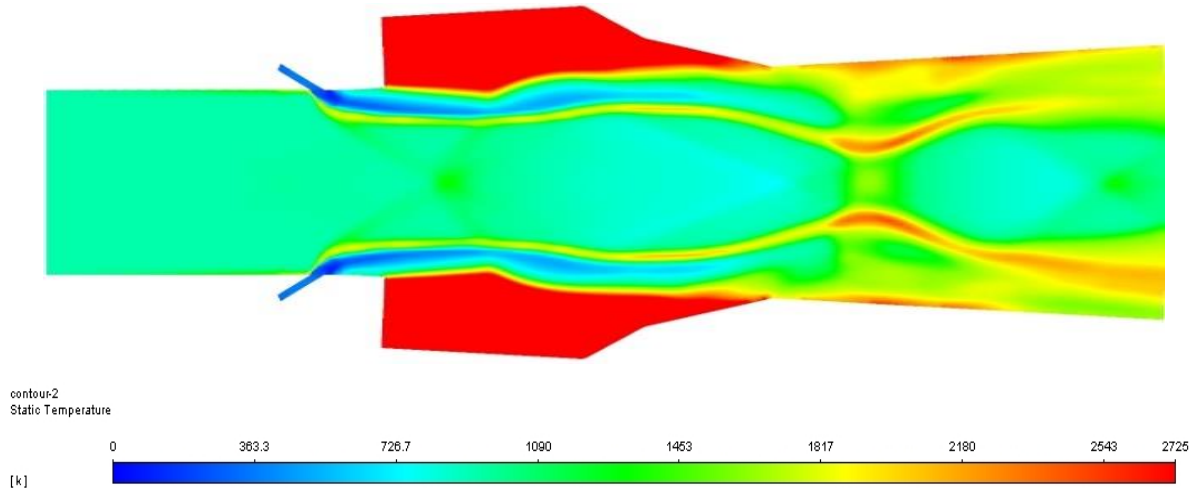

Fig 8. Mean Static Temperature contour at 50 ms

3.4 Vortex Shedding

The influence of the Mach number on turbulence is better understood when analyzing the vorticity equation [14, 15, 16, 17]. By using as reference quantities those at the combustor inlet, that is, u_0 (streamwise velocity component), L_0 (eddy macroscale), $t_0 = L_0/a_0$ (a_0 being the speed of sound), ρ_0, $p_0 = \rho_0 u_0^2$, the non-dimensional equation for vorticity:

$$\frac{1}{M}\frac{\partial \underline{\underline{\omega}}}{\partial} + \underline{\nabla} \times (\underline{\omega} \times \underline{u}) = \frac{\nabla\rho \times \nabla}{\rho^2} + \frac{1}{\mathrm{Re}}\underline{\underline{\nabla^2 \omega}} + \frac{1}{\mathrm{Re}}\left(-\frac{1}{\rho^2}\underline{\nabla} \times (\underline{\nabla} \cdot \underline{\sigma}) + \frac{1}{\rho}\left\{\underline{\nabla} \times \left[\underline{\underline{\nabla^2 u}} + \underline{\nabla}(\underline{\nabla} \cdot \underline{u})\right] + 2\underline{\nabla} \times (\underline{\underline{E}}\underline{\nabla}\boldsymbol{\nu})\right\}\right) \quad (10)$$

$$\frac{1}{\mathrm{M}}\mathrm{I} + \mathrm{CONV} = \mathrm{VS} - \mathrm{CP} + \mathrm{B} + \frac{1}{\mathrm{Re}}\mathrm{DIFF} + \frac{1}{\mathrm{Re}}(-\mathrm{CV} + \mathrm{VV} + \mathrm{DV}) \quad (11)$$

where I, CONV, CP, V S, and B are, respectively, the inertial, convective, dilatational, vortex stretching, and baroclinic terms; DIFF, CV, VV, DV are the diffusive terms due, respectively, to viscous gradients, the coupling between density gradients and viscous stresses, the coupling between viscous stresses and velocity gradients, and the coupling between strain rate and viscous gradients. Equation 11 shows

that in supersonic flows the dilatational term is of the same order of magnitude of the vortex stretching: thus, unlike subsonic flows, vorticity transport is not exclusively driven by vortex stretching, but also by compressibility and baroclinic effects. Further, since the inertial term is proportional to 1/M, when increasing the Mach number, the time dependent so-called "fluctuations" are less and less important and the flow tends to become steady. This equation also suggests that the turbulent kinetic energy transfer from integral to small scales is therefore different from that in subsonic regime, the baroclinic term being a vorticity promoter.

The vorticity can be a significant parameter to quantify the turbulent intensity which improves the fuel-air mixing if it is closer to the shear layer. The following figure represents the vorticity presence within the combustor. The pressure and density gradients regulate the baroclinic term and therefore the vortex transport. In this case, the boundary layer separation has prominently contributed to the vorticity formation towards the shear layer, and shear layer reattachment on the cavity's aft wall amplifies this effect downstream of the cavity. Vortex shedding, which contributes to fuel-air mixing and flame anchoring, is significant.

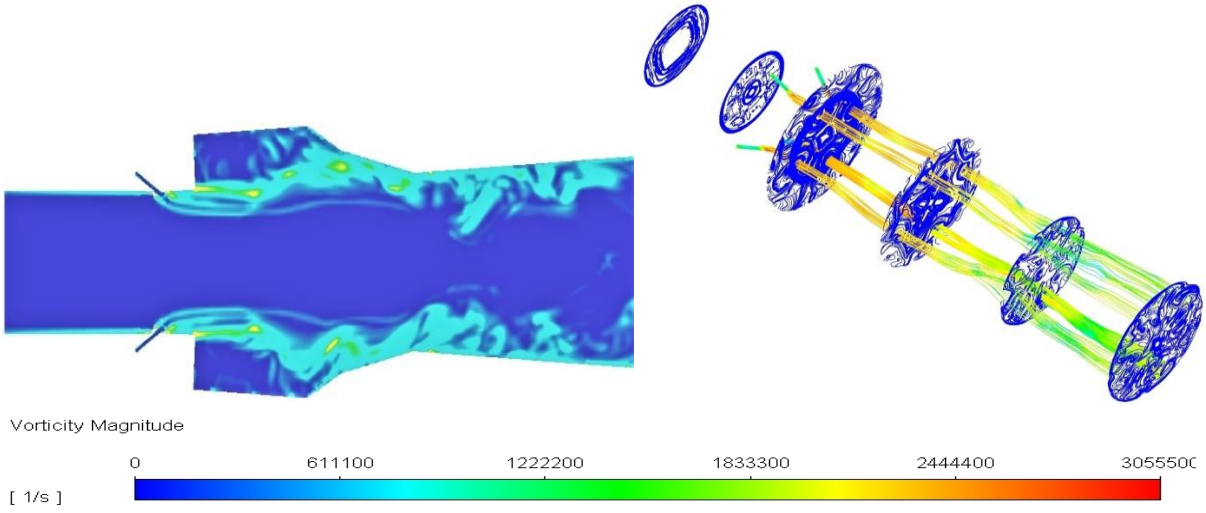

Fig 9. Vortex contour at 50 ms

The Fig. 9 shows that the vorticity is 0 at the inlet and increases to 2.4×10^6 after the fuel injection. Thanks to the vorticity, the mixing time are of the order of 10-3 ms. Vorticity generation may be explained with the baroclinic term: in fact, the high pressure and density gradients and the low hydrogen density, allow its increase and accordingly the vorticity generation.

4. Conclusions

In this work, large eddy simulations of an axisymmetric scramjet engine have been performed. The injection system has been located upstream the cavity, with an angle of inclination of 30°. The injection of hydrogen is responsible for the shock waves formation and the boundary layer separation. Numerical results have shown that the cavity improves the combustion efficiency and acts as a flame holder. Maximum temperatures in the combustion chamber are 2700K. The combustion efficiency is of order of 80 %. Thanks to the baroclinic term, the mixing times are of order of 10^{-3} ms.

References

[1] Yang Z and Zhao X.: Turbulent mixing in supersonic combustion systems. In: 27th aerospace sciences meeting, Reno, NV, 9–12 January 1989. Reston, VA: AIAA.
[2] VanLerberghe, W.M.; Santiago, J.G.; Dutton, J.C.; Lucht, R.P.: Mixing of a Sonic Transverse Jet Injected into a Supersonic Flow. AIAA J. 2000, 38, 470–479..
[3] Fuller, R.P.; Wu, P.K.; Nejad, A.S.; Schetz, J.A.: Comparison of Physical and Aerodynamic Ramps as Fuel Injectors in Supersonic Flow. J. Propuls. Power 1998, 14, 135–145.

[4] Relangi N, Garimella D, Jayaraman K, et al.: Numerical simulations of axisymmetric aft wall angle cavity in supersonic combustion ramjets. AIAA Propuls Energy 2020 Forum 2020; 1–15. DOI: 10.2514/6.2020-3712.
[5] Relangi N, Ingenito A and Jeyakumar S.: The implication of injection locations in an axisymmetric cavity-based scramjet combustor. Energies 2021; 14: 2626.
[6] Relangi N, Ingenito A, Jeyakumar S.: The investigation of inclined AFT wall cavities in a circular scramjet combustor. International Journal of Engine Research 2022:146808742210850. https://doi.org/10.1177/14680874221085059.
[7] Moradi R, Mahyari A, Barzegar Gerdroodbary M, Abdollahi A, Amini Y.: Shape effect of cavity flame holder on mixing zone of hydrogen jet at supersonic flow, Int. J. Hydrogen Energy2018,43, 16364–16372.
[8] Yu, K.H.; Wilson, K.J.; Schadow, K.C.: Effect of Flame-Holding Cavities on Supersonic-Combustion Performance. J. Propuls. Power 2001, 17, 1287–1295
[9] Gruber, M.R.; Donbar, J.M.; Carter, C.D.; Hsu, K.-Y.: Mixing and Combustion Studies Using Cavity-Based Flameholders in a Supersonic Flow. J. Propuls. Power 2004, 20, 769–778.
[10] B. An, M. Sun, Z. Wang, J. Chen.: Cavity flameholding subjected to an expansion fan in a rocket-based combined cycle combustor, Aerosp. Sci. Technol., 106 (2020), Article 106180
[10] A. Ben-Yakar, R.K. Hanson.: Cavity flame-holders for ignition and flame stabilization in scramjets: an overview, J. Propuls. Power, 17 (4) (2001), pp. 869-877
[11] B. An, M. Sun, Z. Wang, J. Chen.: Cavity flameholding subjected to an expansion fan in a rocket-based combined cycle combustor, Aerosp. Sci. Technol., 106 (2020), Article 106180
[11] Gruber, M.R.; Donbar, J.M.; Carter, C.D.; Hsu, K.-Y.: Mixing and Combustion Studies Using Cavity-Based Flameholders in a Supersonic Flow. J. Propuls. Power 2004, 20, 769–778.
[12] Smagorinsky, Joseph (March 1963).: "General Circulation Experiments with the Primitive Equations". Monthly Weather Review. 91 (3): 99–164.
[13] B. An, M. Sun, Z. Wang, J. Chen.: Cavity flameholding subjected to an expansion fan in a rocket-based combined cycle combustor, Aerosp. Sci. Technol., 106 (2020), Article 106180.
[14] A. Ingenito, C. Bruno.: "Physics and Regimes in Supersonic Combustion", AIAA Journal, Vol. 48, No.3, 2010, pp. 515-525, doi: 10.2514/1.43652.
[15] Ingenito A., Bruno, C.: "Mixing and combustion in supersonic reactive flows", 44th AIAA/ASME/SAE/ASEE Joint Propulsion Conference and Exhibit, 2008-45744.
[16] A. Ingenito, D. Cecere, E. Giacomazzi.: "Large Eddy Simulation of Turbulent Hydrogen-fuelled Supersonic Combustion in an Air Cross-Flow", Shock Waves, Vol. 23, 2013, pp. 481-494. doi: 10.1007/s00193-013-0454-7.
[17] Ingenito, A., De Flora, M.G., Bruno, C., Giacomazzi, E., Steelant, J.: A novel model of turbulent supersonic combustion: Development and validation, 2006 Collection of Technical Papers - AIAA/ASME/SAE/ASEE 42nd Joint Propulsion Conference, pp. 423-436.